



Behavior of biocide-free foul control paints for ships' hulls in the immediate proximity of ICCP anodes

F. Castelli, M. Delucchi , F. Valenza, F. Garaventa, M. Faimali, T. Turturro, A. Benedetti

Received: 23 March 2023 / Revised: 20 June 2023 / Accepted: 20 June 2023
© The Author(s) 2023

Abstract Impressed current cathodic protection systems are used in combination with organic coatings to prevent corrosion of hulls. The reaction species which are formed in the proximity of the anodes, like chlorinated compounds and acidity, can stress the antifouling paints of the protective coating system. A 3×3 matrix was defined to drive the tests aiming to investigate the behavior of novel biocide-free foul release (FR) and self-polishing (SP) paints under this kind of attack. The matrix was featured by different pH and free chlorine (free-Cl) values derived by a galvanostatic test performed at an anodic current density required for the protection of paints roughly at their mid age. Chemical/physical characterization was performed through visual analysis, thickness measurements, profilometry, contact angle measurements, and FTIR-ATR analysis. Both FR and SP paints underwent adhesive failure only in the harshest conditions, pH = 3/free-Cl 3–6 ppm, with unmodified chemistry of the polymers. Both paints exhibited no detachment in milder pH/free-Cl conditions, but thick-

ness and contact angle reduction were observed. Finally, results were discussed inferring possible behaviors of the tested paints in real applications.

Keywords ICCP, Foul release paint, Self-polishing paint, Free chlorine, pH

Introduction

Carbon steel, the metallic material by which ship hulls are made of, is easily prone to corrosion in seawater, since this medium is an aerated electrolyte containing several salts, among which NaCl represents the largest fraction (averaging 35 g/L).

To protect hulls from corrosion, active and passive techniques are generally used.

Active techniques consist of maintaining the potential of the hulls at a polarization level where iron oxidation is controlled. This result is achieved making the hull work as a cathode by SACP, sacrificial anodes cathodic protection, or ICCP, impressed current cathodic protection.¹ In the first, electrons are delivered to the hull by galvanic coupling with less noble soluble anodes (usually made of zinc); in the second, the flow of electrons is forced by an electromotive power plant where anodes are insoluble. Passive techniques consist of the application of coatings and paints to the hull surface, aiming to limit the interaction between the metal and seawater. Moreover, at the seawater-paint interface these layers exhibit foul control ability to limit the biofouling development.

Operatively, biofouling can be defined as ‘the unwanted accumulation of biological material on man-made surfaces’ including ‘biofilm-forming microorganisms such as bacteria, fungi, and algae as well as fouling by macroorganisms like hydroids, barnacles, tubeworms, and bivalves on submerged surfaces.’² The biofouling issue, known since ancient

F. Castelli, F. Garaventa, M. Faimali
National Research Council (CNR), Institute of Anthropic Impacts and Sustainability in Marine Environment (IAS), Genoa, Italy

M. Delucchi (✉)
Department of Civil, Chemical and Environmental Engineering, DICCA, University of Genoa, Genoa, Italy
e-mail: marina.delucchi@unige.it

F. Valenza, A. Benedetti
National Research Council (CNR), Institute of Condensed Matter Chemistry and Technologies for Energy (ICMATE), Genoa, Italy

T. Turturro
ACG - Azienda Chimica Genovese s.r.l., Genoa, Italy

times,³ increases the drag, meaning larger fuel consumption, even up to 40–60%.⁴ Since the TBT ban in 2003 due to environmental impacts⁵ and its application stop on ships in 2008,⁶ although this biocide is still used in paint production,⁷ much progress in foul control paints has been made consisting in the development of biocide-free techniques^{8–10} based on superhydrophobicity, microstructuring, switchable features, slippery liquid-infused porous surfaces, SLIPS, etc. In particular, foul release, FR, and amphiphilic self-polishing, SP, coatings, to which this work is devoted, are a market product.

FR coatings allow organisms to adhere weakly, eventually detaching thanks to the water current formed by ship movements.¹¹

The specific FR properties have traditionally been related to the surface hydrophobicity and low energy but are also influenced by other parameters, including surface roughness, elastic modulus, and thickness of the film coating.¹² Amphiphilic self-polishing, SP, coatings exhibit at the surface nanoscale domains with hydrophilic and hydrophobic properties inspired by the microphase separation of structures on the inner wall surface of blood vessels, whose rugged surfaces prevent protein adhesion and thrombus condensation.¹³

Coatings (passive) and cathodic protection (active) techniques coexist with effects related to the involved electrochemical reactions.¹⁴ Especially in case of ICCP plants, cathodic reactions can induce coating disbondment of the coatings^{15–17} due to highly alkaline pH, or H₂ in the case of overprotection. Differently, near the anodes, Cl₂ and H⁺ are delivered into the solution due to the anodic oxidation of Cl⁻ and H₂O providing electrons for the hull protection. A chemical attack up to detachment therefore occurs against the paints near the anode, as reported by producers and users of ICCP systems (see Fig. 1).

Concerning the interaction between active and passive protective techniques, the aim of this work is to evaluate the behavior of FR and SP coatings in the immediate proximity of ICCP anodes. Although this

phenomenon involves a negligible area as low as < 0.01% of the hull surface and does not require a specific intervention until the routinary dry docking hull maintenance, it is interesting to investigate the behavior of these two young coatings in high stress conditions as those near ICCP anodes, where seawater turns locally acidic and chlorinated. To the best of our knowledge, this concern has not been reported yet in the literature.

Referring to the literature,^{18,19} in general, the polymer degradation is defined as ‘any undesirable change in the physical or chemical properties of the polymer as a result of externally applied stimuli.’ Temperature, free chlorine concentration, time exposition and pH are regarded as parameters involved in the polymer degradation in bleaching conditions.^{20, 21}

Here, FR and SP paints were exposed at constant temperature and time to different pH/free chlorine conditions induced by a reference ICCP anodic current density. Chemical and physical properties of the selected paints were evaluated after the treatment.

Experimental

Materials

Two biocide-free foul control paints were analyzed: a foul release, FR, fluoropolymer silicon-based paint, and a self-polishing, SP, amphiphilic paint with microdomain structure.

The specimens were prepared starting from sand blasted steel panels (80 mm × 100 mm × 1.5 mm) painted with an anticorrosive epoxy primer, followed by a specific tie coat for each top coat. The characteristics of the FR and SP painting systems are reported in Table 1.

Twenty-seven specimens for each coating system were prepared.

Tie coat and top coat were applied only on one side of the samples, while the rear was covered by the

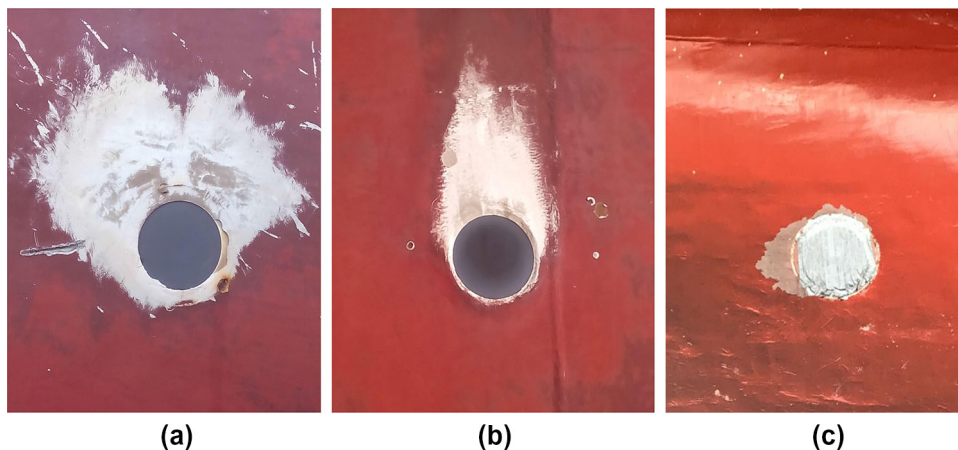


Fig. 1: Failure of paint in areas adjacent to ICCP anodes ($\varnothing = 320$ mm): (a) and (b) after five years, (c) after two years

Table 1: Binder and dry film thickness (DFT) of the coats composing the FR and SP coating systems

	Priming coat		Tie coat		Top coat, FC	
	Binder	DFT (μm)	Binder	DFT (μm)	Binder	DFT (μm)
Coating system1	Epoxy	300	Silicone elastomer	50	Silicone fluoropolymer FR	100
Coating system2	Epoxy	300	Epoxy	75	Micro domain SPC	125

epoxy primer with the same thickness applied on the front side.

All the painted samples were preaged for one month in a 3.5% NaCl solution at 30 °C to leach out any impurities, as suggested by Rahimi et al.²²

Methods

The experiments consisted of the following activities:

- determination of pH and free chlorine, free-Cl, conditions resulting by a galvanostatic polarization,
- 3-month exposition of the FR and SP paints to the determined pH/free-Cl conditions, and
- evaluation of the paints properties after the exposition.

Determination of pH/free-Cl conditions

The pH and free-Cl values necessary to define the pH/free-Cl conditions were determined with galvanostatic polarizations at the operational value of 40 mA cm⁻² for the anodic current density, as suggested by an ICCP installer and by literature.²³

The polarization was performed in a 100-L tank filled with artificial seawater solution (NaCl 23.0 g/L, MgCl₂ · 6H₂O 9.8 g/L, Na₂SO₄ · 10H₂O 8.9 g/L, CaCl₂ 1.2 g/L). A Pt anode was placed in the center of the tank and was polarized at 40 mA cm⁻² for 60 hours. As cathode, a 2.5-mm diameter iron wire was used. The wire was wrapped around the tank to achieve a regular distribution of the current lines.

The pH was monitored at a rate of $\frac{1\text{point}}{5\text{min}}$ with the setup depicted in Fig. 2.

The free-Cl time evolution was monitored collecting 10 mL of solution at 10 mm from the anode, and its concentration was determined with UV-VIS spectrophotometer.

Setup for the exposition to different pH/free-Cl conditions

The setup described in Section “[Determination of pH/free-Cl conditions](#)” allowed for the determination of the pH/free-Cl conditions expected in correspondence

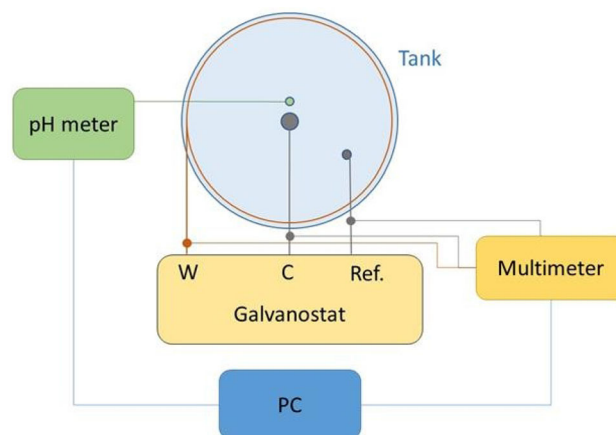


Fig. 2: Experimental setup for the determination of pH/free-Cl values at 40 mA cm⁻². The abbreviations W, C, and Ref. represent the working electrode, the counter electrode, and the reference electrode, respectively

of the areas adjacent to the ICCP anodes, when the ICCP system provides currents typical of mid-aged paints. “pH = 3/free-Cl 3–6 ppm” is the harshest condition, while “pH = 8/free-Cl = 0 ppm” is the reference condition, coinciding with unmodified seawater, away from the anode. Intermediate pH/free-Cl values were defined as well. Hence, nine 60 L tanks for immersion of FR and SP paints were prepared as shown in Fig. 3.

The tanks were placed in the CNR-IAS sea marine station in the Genoa harbor and were filled with natural seawater. The pH < 8 values were obtained adding proper amounts of HCl 1 M; the free-Cl concentrations were reached adding proper amounts of NaClO solution, 15 g/L and 150 g/L (Fig. 4a).

DPD (N,N-diethylparaphenylenediamine) colorimetric test was used for the free-Cl measurements. The pH/free-Cl monitoring and corrections over the three-month experiment were performed 2–3 times a week, accomplishing the following steps: (a) reading of pH and free-Cl; (b) correction with the addition of NaClO through a peristaltic pump controlled by a digital programmable relay in case of drop of the free-Cl concentration (Fig. 4b); (c) control of pH and free-Cl to check shifts from the right values; (d) addition of HCl 1 M up to designed pH values in case of pH shift toward more basic values.

Successively, because of the obtained results, FR and SP painted specimens coming from determined

treatments underwent a physical treatment consisting in a 2-week exposition to a 100% relative humidity at 26 °C atmosphere (100% RH-26 °C); the aim was to reveal possible adhesion loss that occurred during the chemical treatments.

Evaluation of the physical and chemical properties of the paint systems

After the 3-month exposition, all the specimens were rinsed with distilled water and were naturally dried for a few days. The following parameters were evaluated:

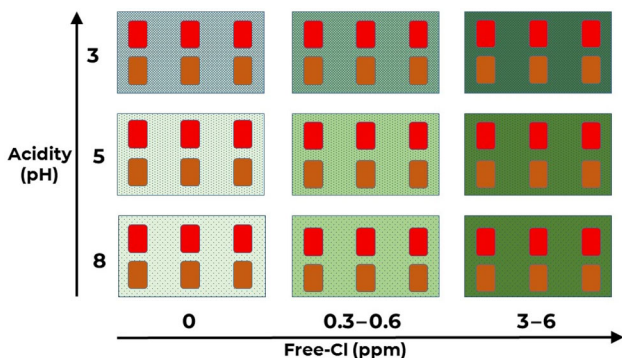


Fig. 3: pH and free-Cl conditions defining the chemical treatments of 60 L tanks filled with natural seawater. The reference condition is “pH = 8/free-Cl = 0 ppm” representing unconditioned seawater, far from the anode. The harshest condition is “pH = 3/free-Cl 3–6 ppm” representing seawater adjacent to the anode in case of large current delivery. The bright and brownish red rectangles represent the FR and SP coatings, respectively

- Paint appearance and detachment evaluation*

Images were collected after 1, 2 and 3 months of exposition and were analyzed using ImageJ software. The macroscopic aspect of the samples was initially evaluated considering possible alterations and color variations. Adhesion reduction is an important factor for the stability of the coatings. Since the chemical composition of FR coatings does not permit the traditional pull-off test, a different procedure was used to evaluate the complete adhesion loss, i.e., blistering occurrence. Therefore, blistering data were collected and elaborated with the aforementioned ImageJ software to obtain the following parameters: (i) number of blisters, (ii) % of blistered area, (iii) blisters area distribution. The three painted panels were evaluated in each pH/free-Cl condition as one undivided specimen. This procedure allowed for highlighting of the time dependence of the paint fraction losing adhesion.
- Thickness*

Thickness measurements were performed on ‘as prepared’ end immersed panels, using a digital dry film thickness (DFT) gauge fitted with a ferrous probe. A grid coordinate system was prepared to define discrete measurement points for the recording of coating thickness, before and after the exposition, in five fixed points in each of the three replica panels in every pH/free-Cl condition. $n = 15$ sized samples were therefore generated for statistical evaluations (paired t test, $p = 0.05$).
- Surface morphology*

The surface features of the applied paints before and after the chemical treatments were quantitatively analyzed and measured with a 3D noncontact profilometer (Sensofar S-neox) using the confocal laser scanning technique. The profilometer is

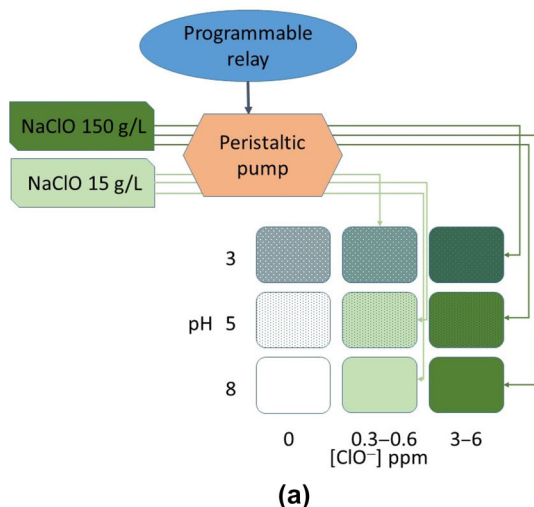


Fig. 4: Experimental setup for the obtainment of the pH and free chlorine, free-Cl, conditions presented in Fig. 3: (a) general scheme; (b) picture of the peristaltic pump for the addition of NaClO and HCl 1 M solution

equipped with three CF60-2 Nikon objectives that allow measurements at different magnification scales, namely 5× (field of view: $3.51 \times 2.64 \text{ mm}^2$; spatial sampling: $2.58 \text{ }\mu\text{m}$; vertical resolution: 75 nm), 20× (field of view: $877 \times 660 \text{ }\mu\text{m}^2$; spatial sampling: $0.65 \text{ }\mu\text{m}$; vertical resolution: 8 nm) and 100× (field of view: $175 \times 132 \text{ }\mu\text{m}^2$; spatial sampling: 0.13 ; vertical resolution: 2 nm). Quantitative measurements of the surface roughness, S_a , according to the ISO 25178 standard, have been performed using the software embedded in the system (SensoSCAN).

- **Contact Angle**

Contact angles were measured achieving the picture of a deionized water drop over the surface with a microcamera. The image was then elaborated with the ImageJ software using a plugin called drop-analysis,²⁴ providing the contact angle (CA) of a low-bond axisymmetric drop by adjusting a line to its contour. $n = 15$ sized samples were achieved on a FR and SP panel before the immersion (references) and were compared with $n = 15$ samples that underwent immersion allowing the statistical evaluation (t test, $p = 0.05$).

- **Chemical integrity**

Possible chemical modification of the surface was evaluated by FTIR-ATR analysis with a PerkinElmer Spectrum Two. Spectra were achieved only on panels immersed in the “pH = 3/free-Cl 3–6 ppm” and on the not exposed specimens (blanks). FTIR spectra were also acquired over the primer in the backside of specimens.

Figure 5 maps the performed investigations.

Results

Determination of the pH/free-Cl conditions

Figure 6 reports the time evolution of pH and free-Cl near the anode in the 40 mA cm^{-2} galvanostatic test. pH oscillated disorderly between 7 and 2–3; these fluctuations likely depend on mass transport phenomena related to bubble gas evolution.^{25–27} About free-Cl, after nearly 8 hours, the concentration reached 1 ppm, while in the successive 48 hours, it increased at a slower rate, staying in the 1–10 ppm range.

These results allowed the determination of the extremes of the treatment range: pH between 3 and 8 and free-Cl between 0 and 3–6 ppm. Hence, “pH = 8/free-Cl = 0 ppm” and “pH = 3/free-Cl 3–6 ppm” were considered, respectively, the reference and the harshest conditions, the first mimicking unconditioned seawater, the second mimicking seawater at the anode/paint interface.

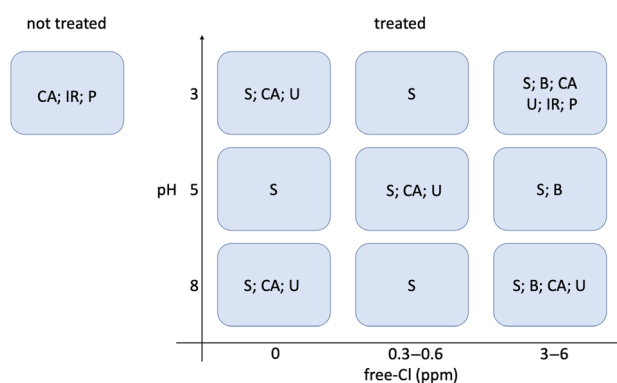


Fig. 5: Map of the investigations performed for the two coating systems, FR and SP: thickness, S; degree of blistering, B; contact angle, CA; 2 weeks exposition to 100% relative humidity-26 °C atmosphere performed after the chemical treatment, U; chemical integrity, IR; profilometry, P

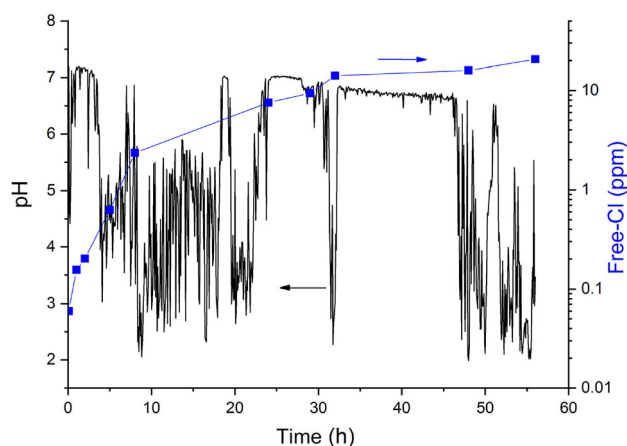


Fig. 6: Measurement of pH (black continuous line) and free chlorine, free-Cl, at 1 cm near Pt anode (blue dotted line) during the galvanostatic polarization at 40 mA cm^{-2} (100 L, NaCl 3.5% wt. solution). See scheme in Fig. 2

Maintenance of the pH/free-Cl conditions

All of the 9 pH/free-Cl treatments define a 3×3 matrix, with reference and harshest conditions being the extremes. The actual time evolution of pH/free-Cl values of the all the nine treatments along the 3 months of exposition is shown in Fig. 7.

Evaluation of the physical and chemical properties of the paint systems

The paint modification was evaluated through a visual inspection of the surface highlighting the integrity and consistency of the paints. Thereafter, blistering degree, thickness, wettability, profilometry and FTIR-ATR spectra were evaluated.

Paint appearance and detachment observation

Figure 8 shows the appearance of the FR and SP paints after the 3-month exposition to the different pH/free-Cl conditions.

The blistering appeared evident only for the FR paint exposed to the “free-Cl 3–6 ppm” treatment at all the pH values. In turn, the polymer of the SP paint became softer and easier to scratch with respect to the beginning of the exposition.

In Fig. 9, the number of blisters and the % of blistered area are reported in function of the immersion time. A pH dependence was observed; the more acidic the pH, the lower the number of blisters and the larger the blistered area.

A finer analysis of the data is reported in Fig. 10.

The box-plot distributions of the blistered areas in pH = 8, 5, 3 evolving along 3 months are presented in Fig. 10a–c, respectively. Being (i) the median of the blisters area the value below which 50% of area values are found, (ii) the mean of the blisters area computed considering all the area values, the difference (mean–median), M, weights larger blister areas.

In Fig. 10d–f, the monthly evolutions of M for each pH are presented, which are analytically fitted with an asymptotic model at pH = 8 ($r^2 = 0.947$, Eq. 1), polynomial second-order model ($r^2 = 0.998$, Eq. 2) at

pH = 5, exponential model at pH = 3 ($r^2 = 0.999$, Eq. 3).

$$M(t)_{pH=8} = 0.136 - 0.136 \times 0.212^t \tag{1}$$

$$M(t)_{pH=5} = -0.075 + 0.4t + 0.9t^2 \tag{2}$$

$$M(t)_{pH=3} = -0.378 + 0.378 \times e^{\frac{t}{0.564}} \tag{3}$$

The derivative $\frac{dM}{dt}$ at each pH (Fig. 10g–i) describes the speed at which M evolves; in other words, how rapidly larger blisters increase. It is evident how pH affects the development of larger blisters tuning the evolution rate from exponential decrease, at pH = 8, to exponential increase, at pH = 3. The decrease in the number of blisters (Fig. 9a) in parallel to the increase in % of blistered area (Fig. 9b) means blisters coalescence, resulting in paint detachment. Therefore, results in Fig. 10 reveal that when free-Cl > 3 ppm, the paint detachment is highly promoted when pH turns acidic.

Thickness

Figure 11 presents the following parameters:

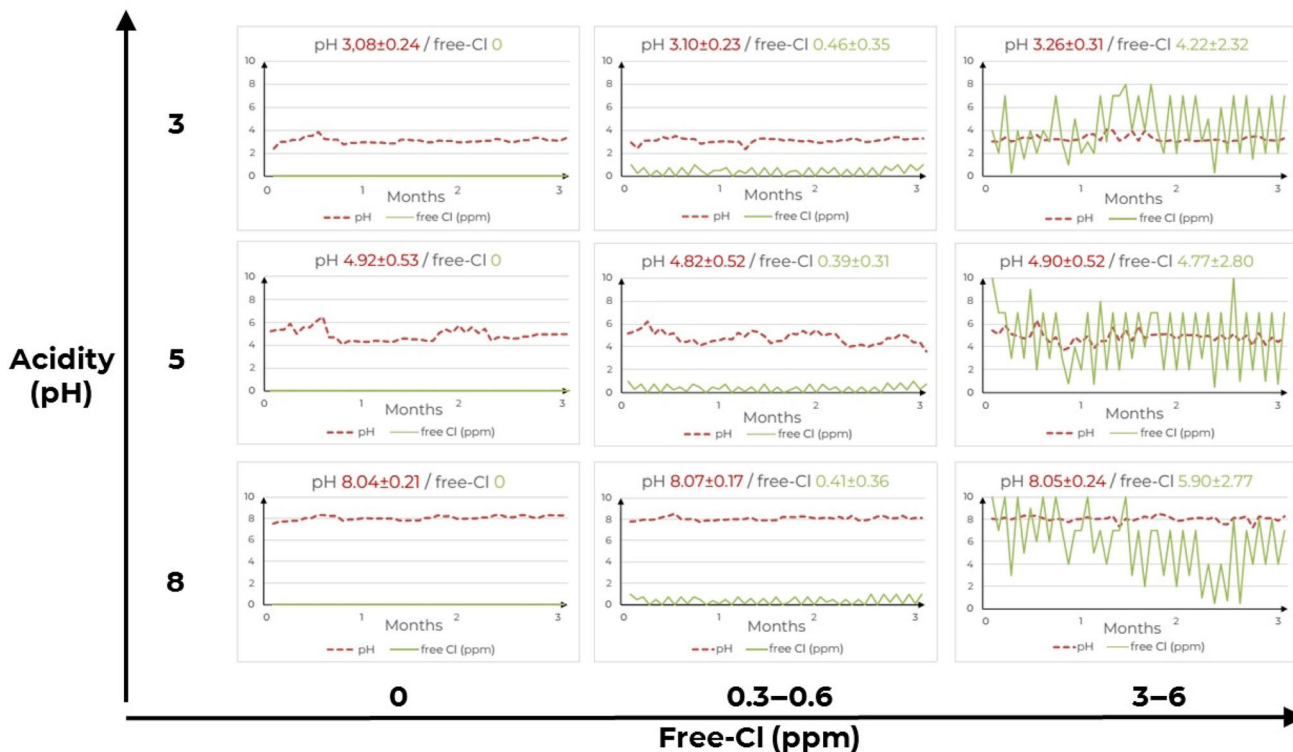


Fig. 7: Actual time evolution of pH and free-Cl for the nine solutions with nominal pH = 8, pH = 5, pH = 3 and nominal free-Cl concentrations of 0, and in the ranges 0.3–0.6 and 3–6 ppm. In the head of each graph is indicated the mean ± s.d. of measured pH and free-Cl data along the 3-month expositions

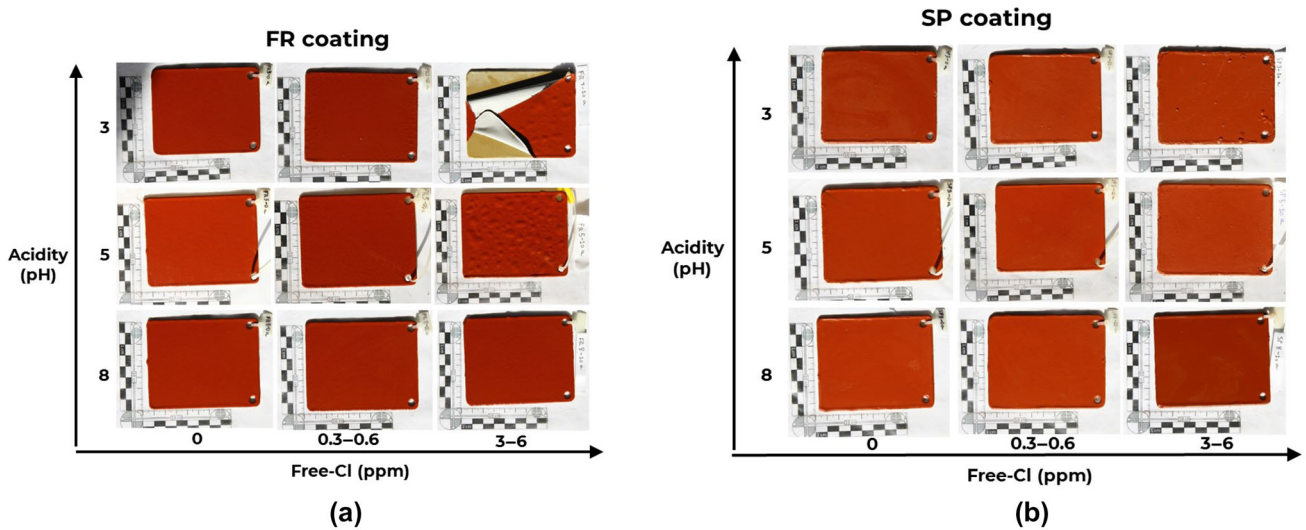


Fig. 8: Appearance of the panels painted with (a) FR and (b) SP coatings after exposition for 3 months to the different pH/free-Cl conditions summarized in Fig. 3

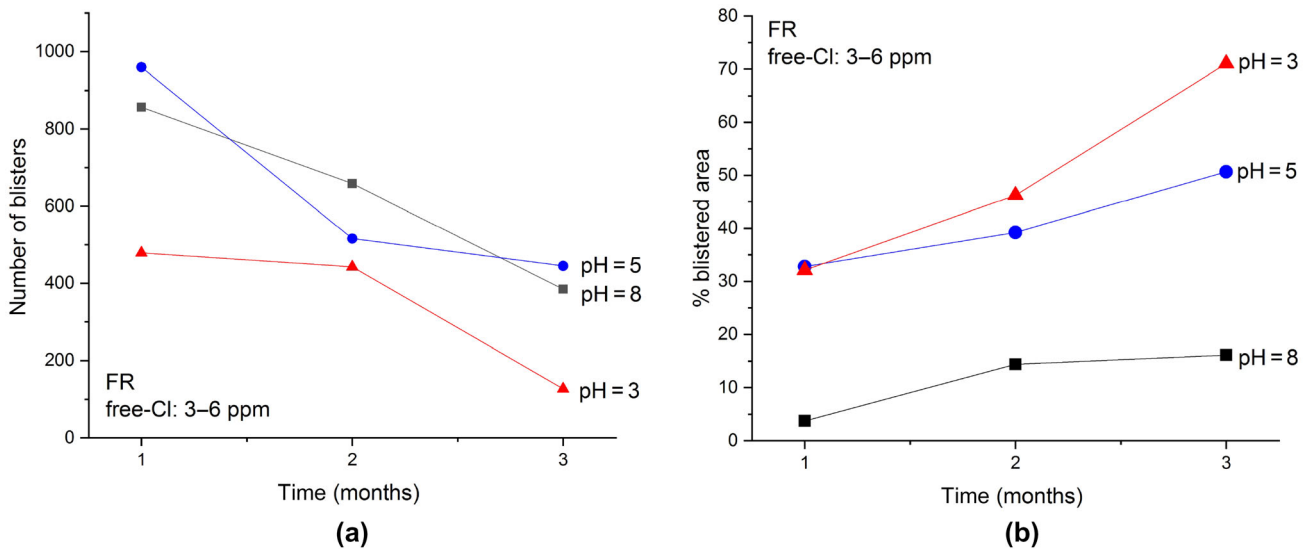


Fig. 9: FR paint exposed to the harshest free chlorine concentration (3–6 ppm). Time evolution of: (a) number of blisters; (b) % of blistered area

- $S_{pre} \pm \sigma$ (μm), representing mean \pm s.d of the thickness value before immersion for $n = 15$ sized samples,
- $S_{post} \pm \sigma$ (μm), representing mean \pm s.d of the thickness value after immersion for $n = 15$ sized samples,
- $\Delta\%$, representing the percentage difference between S_{pre} and S_{post} .

In the reference “pH = 8/free-Cl = 0” condition, neither FR nor SP paints suffered statistically significant thickness reduction. For FR paint, with chemical treatments featured by pH < 8 and free-Cl > 0 ppm,

the thickness reduction increased with the strength of the treatment reaching up to 4.75% in the harshest conditions. For the SP paint, the thickness difference was statistically significant only at pH = 5 and pH = 3 with free-Cl = 3–6 ppm, with 0.9 and 2.2% thickness reduction, respectively.

Roughness

The not immersed surfaces of FR and SP samples were compared with surfaces immersed in the harshest pH/free-Cl conditions.

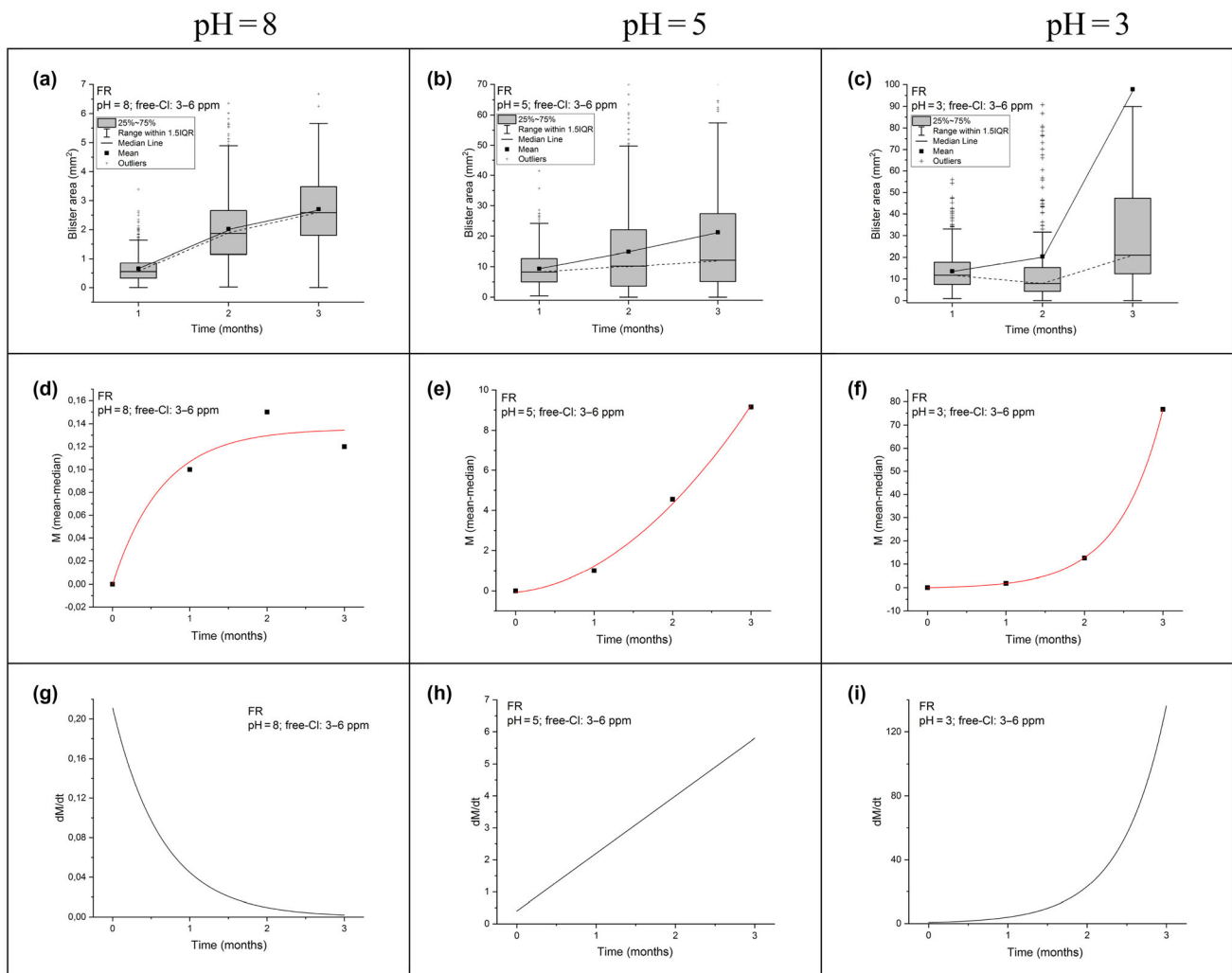


Fig. 10: Time evolution of the box-plot distributions relative to the areas of blister in free-Cl 3–6 ppm for (a) pH = 8; (b) pH = 5; (c) pH = 3. Time evolution of the difference $M = \text{mean} - \text{median}$ (red line fitting model of $M(t)$) in free-Cl 3–6 ppm for (e) pH = 8; (f) pH = 5; (g) pH = 3. Time evolution of $\frac{dM}{dt}$ in free-Cl 3–6 ppm for (g) pH = 8; (h) pH = 5; (i) pH = 3

The 3D reconstruction of the surface of the FR paint is shown in Fig. 12. The surface appeared wavy at the naked eye, and this feature can be noted looking at low magnification profiles and Sa values (Fig. 12a1, a2). On the other hand, higher magnification profiles (Fig. 12a3) evidenced that the surface is actually very smooth (see Table 2), as confirmed by Sa values laying in the 10–100 nm range. The 3D reconstruction of the surface of the SP paint is shown in Fig. 13. Before immersion, the surface appeared rough (Fig. 13a1–a3) as demonstrated by Sa values (Table 2). The 3-month immersion induced a further roughening level. In addition, the formation of holes was detected (Fig. 13b1–b3).

Data in Table 2 show that at the highest magnification (100×) FR paint exhibits the smoother surface which was basically unmodified after the treatment, with Sa before the chemical treatment being 0.036 μm

and 0.054 μm after the treatment. At the same magnification, SP exhibited roughly tenfold higher Sa, which increased from 0.22 μm to 0.27 μm. This variation is supposed to depend on the holes observed after the treatment. At lower magnifications, 20× and 5× the FR and SP paints exhibit an apparently similar behavior, since Sa (i) is in the same order of magnitude and (ii) increases after the treatment. It is possible that roughness values are influenced by the presence of residual scraps left after the chemical treatment or that the treatment induced a slight swelling in relation to the observed thickness variations (Fig. 11).

Hydrophobicity

Figure 14 presents the following parameters:

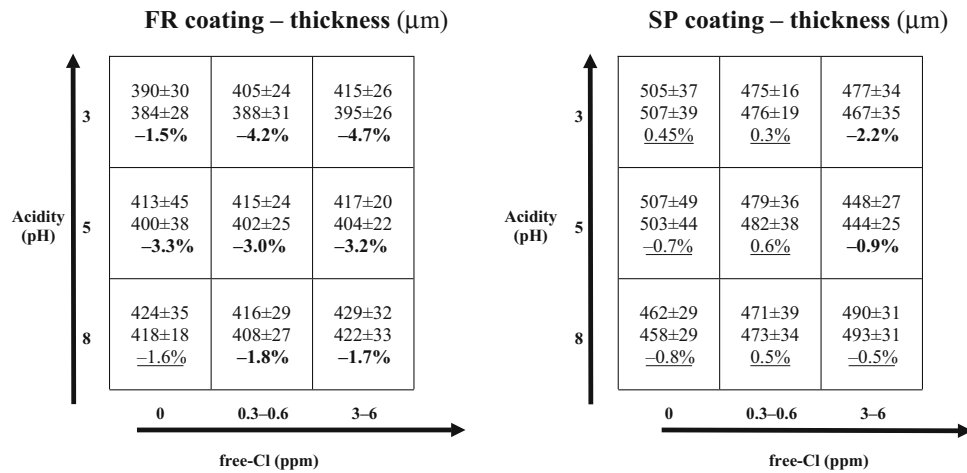


Fig. 11: Thickness values (µm) $S_{pre} \pm s.d.$, $S_{post} \pm s.d.$ (first and second number in each cell, respectively) before and after the 3-month immersion and $\Delta\%$ values after the immersion (third number in each cell) in different pH/free-Cl chemical treatments. Bold and underlined values represent statistically significant (p value < 0.05) and not significant (p value \geq 0.05) variations

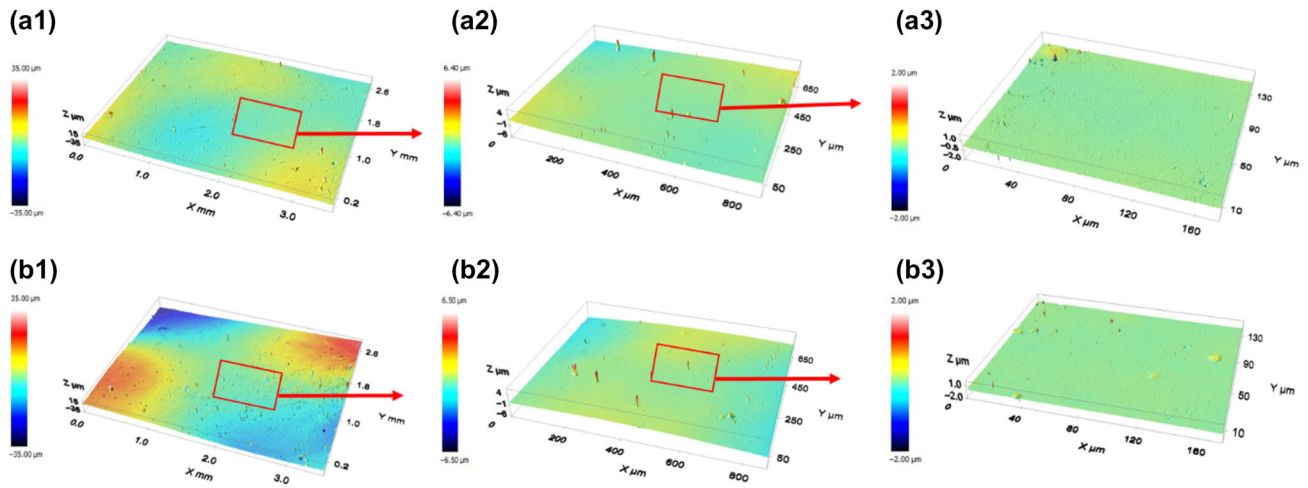


Fig. 12: Three-dimensional reconstruction of surface scans of the FR paint before (line a) and after (line b) the 3-month treatment at “pH = 3/free-Cl 3–6 ppm” at different magnifications (5×; 20×; 100×)

Table 2: Sa values by profilometry on SP and FR paints before/after the chemical treatments summarized in Fig. 3

Sample		5× (3.51 × 2.64 mm ²)	20× (877 × 660 µm ²)	100× (175 × 132 µm ²)
FR	Sa before treatment	2.84 µm	0.30 µm	0,036 µm
	Sa after treatment	7.28 µm	0.56 µm	0,054 µm
SP	Sa before treatment	3.17 µm	0.66 µm	0.22 µm
	Sa after treatment	7.45 µm	0.87 µm	0.27 µm

- $CA_{ref} \pm \sigma$ ($^{\circ}$), representing mean \pm s.d. of the CA reference value obtained before the immersion for $n = 15$ sample. This value is used as reference to compare the CA data after the chemical treatment,
- $CA_{post} \pm \sigma$ ($^{\circ}$), representing mean \pm s.d. of the CA values after the chemical treatments for $n = 15$ sized samples,
- $\Delta\%$, representing the percentage difference between CA_{ref} and CA_{post} .

Neither FR nor SP paints suffered statistically significant CA modification when immersed in the

reference chemical treatment. For FR paint immersed in $pH < 8$ and free-Cl > 0 ppm conditions, CA decreased with the increase in acidity and free-Cl, up to a -9.6% variation in the harshest condition. For the SP paint, the CA decrease was induced by the free-Cl increase and acidity decrease, up to -16.6% in the harshest condition. Nevertheless, the largest CA variation of -25.7% was obtained in the “pH = 8/free Cl 3–6” chemical treatment. Hence, for both FR and SP paints, the CA reduction was driven by increasing free-Cl, but with opposite effects in relation to pH.

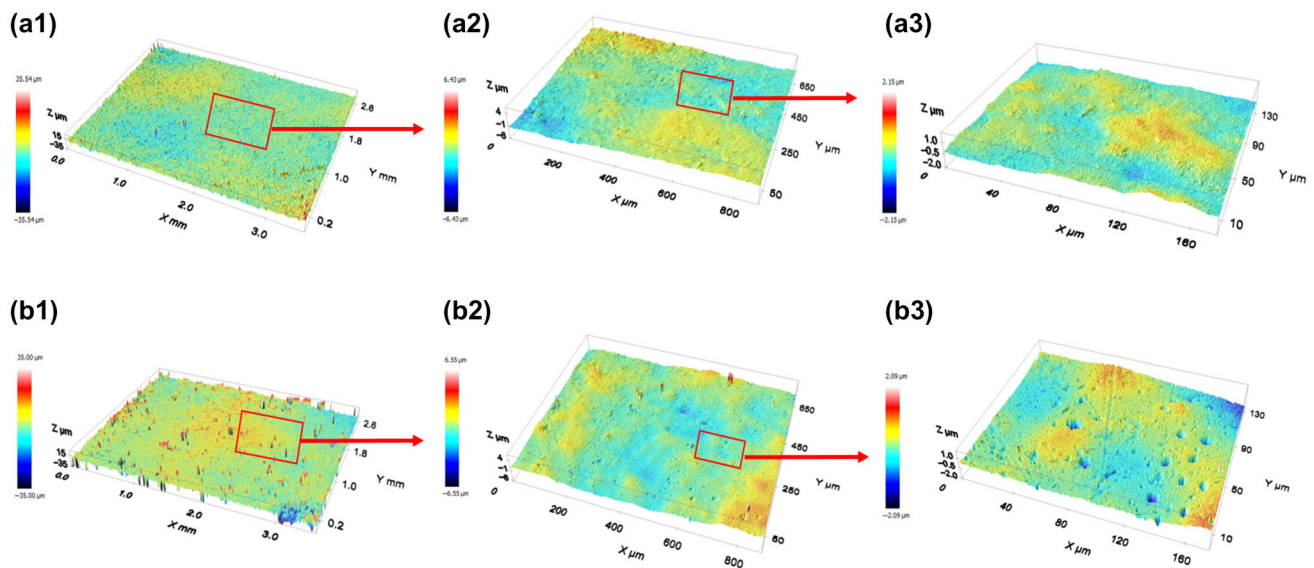


Fig. 13: Three-dimensional reconstruction of surface scans of the SP1 paint before (line a) and after (line b) the 3-month treatment at “pH = 3/free-Cl 3–6 ppm” at different magnifications (5×; 20×; 100×)

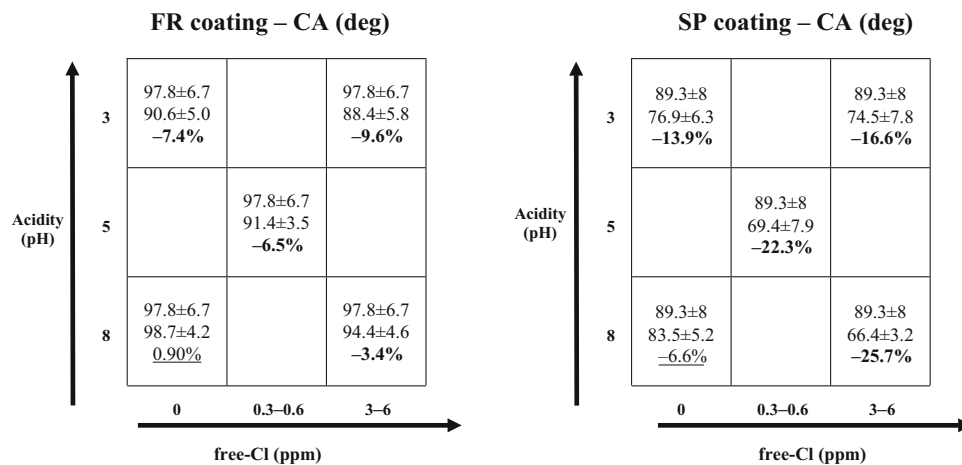


Fig. 14: Contact angles: $CA_{ref} \pm \sigma$ and $CA_{post} \pm \sigma$ (first and second number, respectively, in each cell) are the values before (reference) and after the 3-month immersion in different pH/free-Cl chemical treatments. $\Delta\%$ is the percentage difference (third number in each cell). Bold and underlined values represent statistically significant (p value < 0.05) and not significant (p value ≥ 0.05) variations.

Chemical integrity

FTIR spectra were achieved for the FR (Fig. 15) and SP (Fig. 16) paints exposed to the harshest treatment to evaluate possible chemical modifications in comparison with not exposed specimens ('external blank').

No chemical modifications of the foul control top coats were evident. In turn, the epoxy primer suffered bleaching (Fig. 17).

Figure 18 shows the spectra obtained on the epoxy primer of the samples reported in Fig. 17.

In the not exposed epoxy primer, peaks at 1507 cm^{-1} and 1180 cm^{-1} are clearly visible. In specimens exposed for 3 months to the harshest "pH = 3/free-Cl 3–6 ppm" condition (Fig. 17b), these peaks are missing, or their relative intensity is reduced. The large blistering of the FR top coat allowed observation of the epoxy layer beneath (Fig. 17c), which resulted as bleached as the epoxy layer in the back side (Fig. 17a), indicating the permeation of oxidizing agents through the FR top coat. The spectra obtained in these areas present these peaks but attenuated.

Regarding SP paint, only the specimens exposed to the harshest treatment exhibited a large swelling (Fig. 19) after exposition to the 100%RH-26 °C treatment: the top coat detached from the tie coat, while the tie coat seemed to adhere well to the epoxy primer. No other paint coming from any other chemical treatment showed a similar detaching and swelling behavior after the 100%RH-26 °C treatment.

The detaching events regarding the FR and SP paints after the chemical and physical treatments are shown in Fig. 19.

Summary of the results

Results of FR and SP exposition to different pH/free-Cl conditions are summarized as follows.

- FR: Blistering was observed at the epoxy primer/tie coat interface in the highest free-Cl concentration along the three values of pH, with the most acidic

pH being the most degrading. The thickness decreased by 4.7% in the harshest conditions. Hydrophobicity decreased up to 9.6 % mainly due to interfacial chemistry at the weaker bond level.

- SP: No blistering was apparently observed after the 3-month chemical treatment. In turn, the top coat exposed to the harshest conditions was detached at the tie coat–top coat interface after a successive 2-week exposition in a 100%RH-26 °C atmosphere. In the harshest conditions, the thickness was reduced by 2.2%. Hydrophobicity decreased by 16.60% with a contribution of the superficial rugosity increase.

IR data indicated that no chemical modifications were evident for both the FR and SP top coats.

Discussion

The discussion is divided in two sections: the first regards the results of the chemical attack on the selected paints, and the second regards the interpretation of these results in the framework of real applications.

Thickness reduction, blistering, and detachment

In the harshest conditions, (top right cell of the matrix in Fig. 3), FR paint suffered the worst thinning, blistering, and hydrophobicity reduction. About thickness, free-Cl or acidity determined alone no more than $\sim 1.5\%$ reduction, while when cooperating, they determined 4.7% reduction. The volume diminution, in different conditions, features drying or curing stages.^{28–30}

Here, thickness reduction in the FR paint coincided likely with a volume diminution rather than a mass loss, as suggested by the chemical inertness of the polymer. In turn, the 2.2% thickness loss observed for the SP paint coincides rather with a mass loss due to the ablating nature of the SP paint itself. As by data in

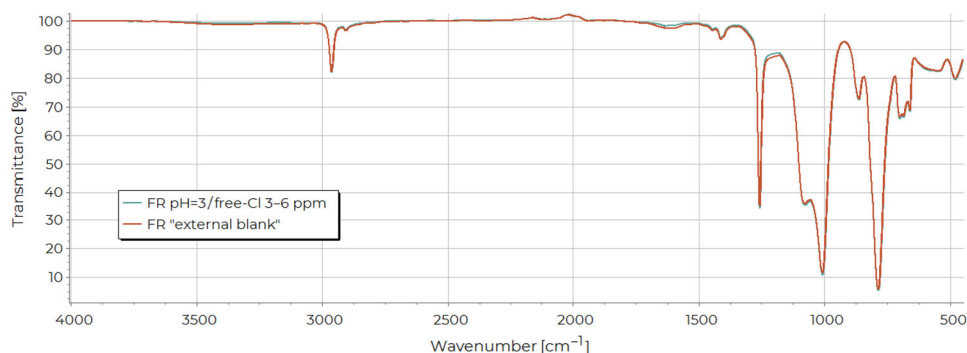


Fig. 15: FTIR spectra of the FR paint not exposed and exposed for 3 months to the harshest treatment, "pH = 3/free-Cl 3–6 ppm"

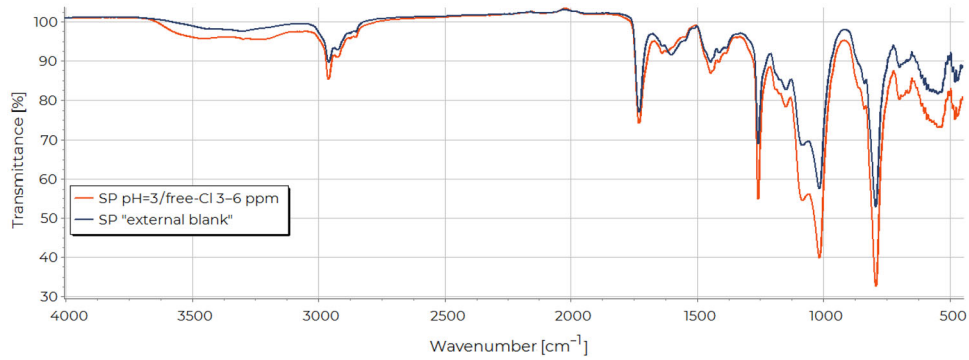


Fig. 16: FTIR spectra of the SP paint not exposed and exposed for 3 months to the harshest treatment, “pH = 3/free-Cl 3–6 ppm”

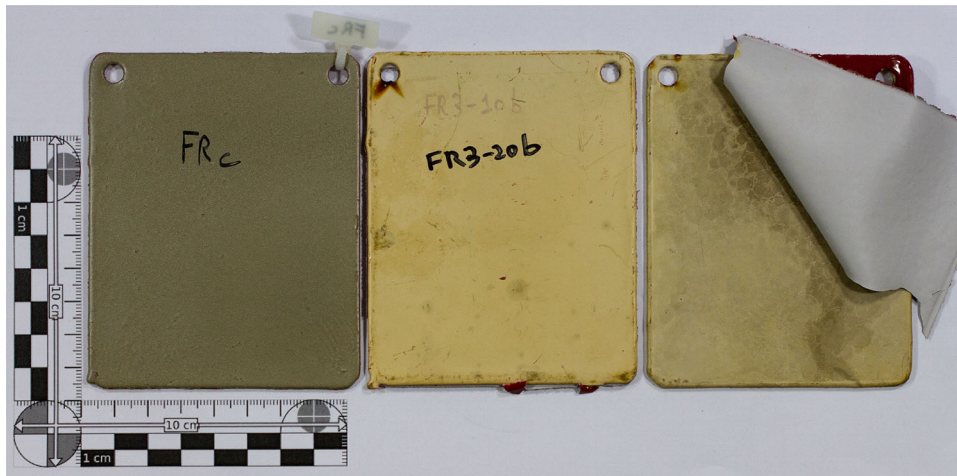


Fig. 17: (a), (b) rear view of a specimen painted only with the epoxy primer not exposed and exposed for 3 months to the harshest treatment “pH = 3/free-Cl 3–6 ppm,” respectively. In (b), bleaching is evident; (c) front view of a specimen painted with the FR top coat, exposed for 3 months to the harshest treatment “pH = 3/free-Cl 3–6 ppm”; the detachment of the ‘tie coat + top coat’ layers and the bleaching of the primer are evident

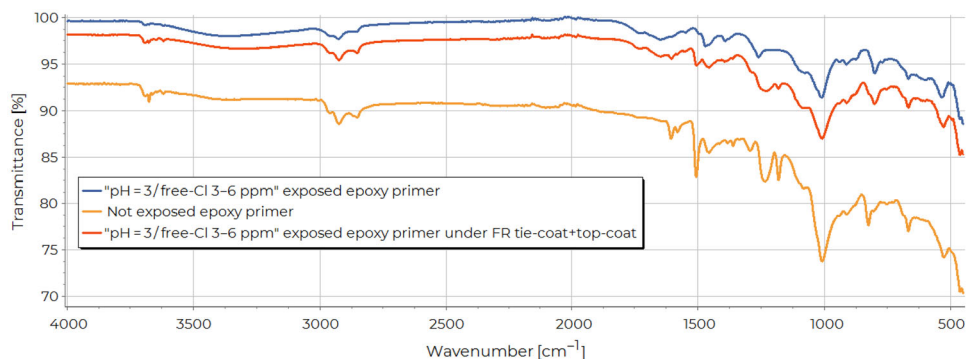


Fig. 18: FTIR spectra obtained on the epoxy primer in different conditions

Fig. 11, free-Cl appears to be the only thinning cause operating more successfully as pH decreases. Specimens exposed in the reference “pH = 8/free-Cl = 0 ppm” condition did not exhibit statistically relevant thinning: probably, the polishing rate in the reference-like condition is negligible over a 3-month period. The

2.2% loss of the 125 μm top layer in the harshest condition implies an average polishing rate of about 1 μm month⁻¹, which is lower than 10–15 μm month⁻¹ rates obtained using a laboratory rotor at room temperatures.³¹ Hence, for the SP paint, chemical oxidation by NaClO induced an increase in the

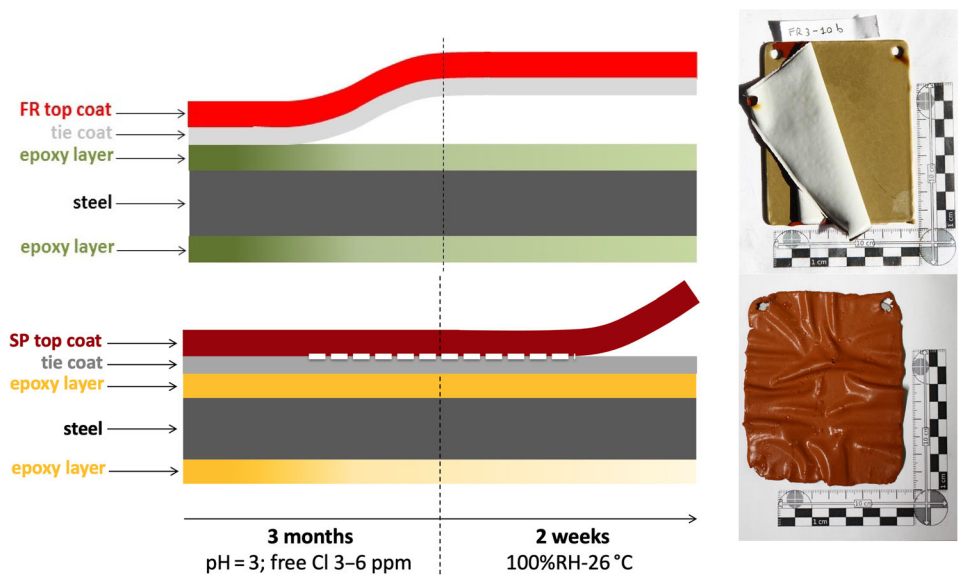


Fig. 19: Scheme of detaching events on FR and SP paints after the 3-month exposition in the harshest treatment “pH = 3/ free-Cl 3–6 ppm,” and, successive 2 week physical treatment, 100% RH-26 °C. The dotted line at the interface between the top coat and the epoxy layer of the SP paint means that detaching occurred during the chemical treatment and was revealed during the physical one. The fading color of the epoxy layer represents bleaching

polishing rate equivalent to a modest but not negligible fraction with respect to merely mechanical effects.

Thickness reduction due to chemical attack has been reported by other authors too,³² evidencing that easier detachment occurred on some paints exposed to the Cl₂ by-products produced by the anode. Nevertheless, whether the thickness reduction observed here helped detachment phenomena cannot be argued; further investigation would be needed.

Regarding detachment, FR blistered in the free-Cl 3–6 ppm condition, with acidity acting as accelerating factor (Figs. 9, 10). Differently, SP paint exhibited swelling and detachment during the 2 weeks of physical treatment at 100%RH-26 °C after the 3-month chemical treatment in the harshest condition. Hence, for both FR and SP paints, acidity helped free-Cl to determine blistering and detaching effects. FTIR shows that polymers of the FR and SP paints were not affected by the chemical attack (Figs. 15, 16), which, in turn, affected the epoxy primer beneath the FR paint (Fig. 17, side 2). Therefore, the hypothesis relies on NaClO-related oxidants permeation through the polymer reacting with the matrix at a slower rate with respect to the reaction occurring at the interfaces, where detachments were observed (Fig. 17, side 3).

Data available in the literature are those regarding the polishing of filtration membranes with NaClO. Its concentration, *C*, provided for a certain amount of time, *T*, defines the chemical treatment, *CT* (ppm × h)³³:

$$CT = \int C(t)dt \tag{4}$$

Our NaClO delivery procedure did not allow an easy determination of the chemical treatment as suggested by Eq. 4, but allowed determining the chemical attack, *CA*, by the free-Cl over the period *T*,¹⁴ i.e., the 3-month exposition. A comparison between literature *CT* data and *CA* data achieved here can be made determining, (i) the theoretical equivalent NaClO concentration, *C_e*, from free-Cl data and (ii) the equivalent chemical treatment, *CT_e*, integrating *C_e* over *T*.

At pH = 3, *C_e* is:

$$C_e(\text{free Cl}) = \left\{ \frac{\%_{Cl_2} \cdot [\text{free Cl}]}{MW_{Cl_2}} n_{Cl_2} + \frac{\%_{HClO} \cdot [\text{free Cl}]}{MW_{HClO}} n_{HClO} \right\}_{pH=3} \times MW_{NaClO} \tag{5}$$

Being

%_{Cl₂}: the Cl₂ percentage at pH = 3, i.e., 30%,³⁴
%_{HClO}: the HClO percentage at pH = 3,³⁴ i.e., 70%,
 [free Cl]: free-Cl concentration measured with DPD,
MW_{Cl₂}: Cl₂ molecular weight, 70.9 g mol⁻¹, *MW_{HClO}*: HClO molecular weight, 52.460 g mol⁻¹, *MW_{NaClO}*: NaClO molecular weight, 74.44 g mol⁻¹, *n_{Cl₂}*: one mole of Cl participating to the DPD reaction, provided by one mole of Cl₂, $\frac{1 \text{ mol Cl}}{1 \text{ mol Cl}_2}$, *n_{HClO}*: one mole of Cl participating to the DPD reaction, provided by one mole of HClO, $\frac{1 \text{ mol Cl}}{1 \text{ mol HClO}}$,

Analogously to Eq. 4, it is:

$$CT_e = \int C_e(t)dt \tag{6}$$

Considering that at pH = 3, the mean value for free-Cl concentration is 4.22 ppm (see Fig. 7), by Eq. 5, it is $C_e = 4.9$ ppm. With $T = 3$ months corresponding to 2160 hours, by Eq. 6, it is $CT_e = 1.06 \times 10^4$ ppm \times h.

Chemical modifications on polymers of filtering membranes have been found along the CT range 10^4 – 10^7 ppm \times h.^{33, 35–38} Here, detachment occurred without chemical modifications for both FR and SP paints in the harshest conditions, with $CT_e \approx 10^4$ ppm \times h (see column 3–6 ppm free-Cl). The works of Devilliers et al.³⁹ and Mikdam et al.³⁴ are helpful, remembering that the $Cl_2/HClO/ClO^-$ ratios are tuned by pH, so that, Cl_2 and $HClO$ are prevalent for pH < 5.

Mikdam et al.³⁴ provided evidence how Cl_2 ‘can directly dissociate into Cl^\bullet and OH^\bullet radicals’ for pH < 7, which are able to penetrate the polymer matrix:



OH^\bullet , is likely scavenged in the most superficial layers of the polymer due to its largest reactivity, while Cl^\bullet is expected to penetrate deeply at a slower rate. Mikdam ascertained the oxidative role of chlorinated radicals. Devilliers et al.³⁹ aged polyethylene in chlorine solutions with $CT = 4.7 \times 10^5$; 10^6 ; 3.36×10^6 ppm \times h, hypothesizing the role of less reactive species such as Cl_2OOH to be responsible for the observed degradation, acknowledging the unclearness of the real mechanism.

Finally, $CT_e \approx 10^4$ ppm \times h does not exclude in the case of polymers for filtering membranes a chemical attack by free-Cl, which was not observed on FR and SP polymers likely because of their larger chemical stability, as witnessed by FTIR data. Therefore, paints detachment appears to be induced by the permeation of Cl reactive species targeting chemical bonds at the adhesive interfaces. As a matter of fact, these consist of dipole–dipole, van der Waals forces, ionic, covalent, metallic bonding, involving polar groups⁴⁰ and radicals too,⁴¹ more prone to be attached once reached.

Contact angle, profilometry

Surface free energy of a solid surface S, γ_S (mJ m⁻²), is an important parameter governing the foul control properties, especially for FR paints, for which the weakening of bio-adhesion by low surface energy has been known for decades.^{42, 43} This property, along with the surface geometry (rugosity), affects the apparent water contact angle, ϑ_a .

Combining the Young’s equation for the relation between the static contact angle on smooth solid surface, ϑ_0 , and γ_S

$$\cos \vartheta_0 = \frac{\gamma_S - \gamma_L}{\gamma_{SL}} \tag{9}$$

with the Wenzel equation for the geometry surface in the regime of homogeneous wettability.⁴⁴

$$r = \frac{\cos \vartheta_a}{\cos \vartheta_0} \tag{10}$$

the relation between ϑ_a and γ_S can be so derived, as suggested by Han et al.⁴⁵:

$$\cos \vartheta_a = r \times \frac{\gamma_S - \gamma_L}{\gamma_{SL}} \tag{11}$$

Equation 11 shows that wettability (as $\cos \vartheta_a$) is directly related to γ_S (being γ_{SL} and γ_L the solid/liquid interfacial tension and water surface tension, respectively), and weighed by the geometric surface of the solid S, expressed by r . Here, ϑ_a decrease (see Fig. 12) shows that the chemical treatment affected interfacial properties of both the FR and SP paints, increasing the hydrophilicity (wettability).

As mentioned in “[Interpretation of the results in the framework of real applications](#)” section, SP paints after treatment exhibited the formation of holes resulting in an increase in surface roughness (see the profilometry results in Fig. 13). Hence, the enhancement of wettability likely depends on a more complex surface geometry too, described by the factor r in Eq. 10. In the literature, it is reported that the surface geometry modification after chemical treatment on polymers of different nature shifts CA toward hydrophilic angles.^{46, 47}

In turn, similar evaluations seem not to regard the FR paint, for which the profilometry results showed basically a stability of the geometric features at the higher magnification. Hence, especially for the FR paint, the slight wettability increase seems to depend basically on variation of the interfacial chemistry. IR spectra in Figs. 16 and 17 showed that no chemical modification occurred at the level of the covalent bonds, but other changes might have occurred on weaker ones. This evidence agrees with the γ_S composition by apolar γ^{LW} and polar γ^{AB} components, $\gamma_S = \gamma^{LW} + \gamma^{AB}$, being Lewis acid-base pairs (AB) and van der Waals (LW) bonds of lower energy with respect to covalent ones.^{48, 49}

To sum up, the wettability increase with the intervention of the factor r for the SP paint seems to be in line with its ablative nature. The chemical attack stimulates polishing phenomena increasing the roughness as witnessed by holes visible at the largest magnification (Fig. 13-b3), therefore contributing to the increase in the wettability. Conversely, the enhancement of wettability for the FR paint would potentially limit its foul control performances.

Hence, for both FR and SP paints, the chemical acidic/chlorinated attack related to anodic-like elec-

trochemistry results in enhancement of the wettability despite the basic stability of the polymeric chemical structure.

Interpretation of the results in the framework of real applications

In Sections “**Thickness reduction, blistering, detachment**” and “**Contact angle, profilometry**,” it is discussed how FR and SP paints react to a chemical stress in different pH/free-Cl conditions imposed for three months, taking as a starting point what happens near ICCP anodes. To interpret the results obtained in laboratory conditions with respect to real operative ones, it is necessary to recall how the impressed current cathodic protection system works.

The ICCP system intervenes delivering cathodic current to the hull when its potential reaches values nobler than + 220 mV vs Zn. The current delivery depends on the protection current demand, which is related to the paint state and the hydrodynamic regime combining mooring vs sailing stages. At a finer geometrical scale, different parts of the ship feel different hydrodynamics during sailing. Basically, equal to the hydrodynamic regime, younger paints imply less protection current requirement, while aged paints imply larger protection current. Equal to the paint state, larger water turbulence implies larger current requirement.

Regarding anodes for ICCP plants, these are featured by different current supply thresholds, A_t (A) and diameters in case of circular shapes, \varnothing (mm) depending on the ship and hull surface to be protected. As reported by an installer of ICCP plants with circular MMO anodes, the (A_t ; \varnothing) interval ranges from $A_t = 50$ A; $\varnothing = 110$ mm to $A_t = 200$ A; $\varnothing = 470$ mm. Here, a $A_t = 100$ A, $\varnothing = 320$ mm anode has been considered as reference, since it lays in the middle of the aforementioned interval and is largely used. Hence, based on the $\varnothing = 320$ mm anode, during the first year (young paint), 10–20% of the $A_t = 100$ A threshold is averagely required, during the second year around 40%, then not over 80% until the drydock, when the paint is more aged. Assuming 800 cm^2 to be the nominal surface of the reference $\varnothing = 32$ mm MMO anode, the operative range for the anodic current density, i_{an} , lays in the 10–100 mA cm^{-2} range.

Hence, the value of 40 mA cm^{-2} , which was used to infer the pH/free-Cl values near the anode, is somehow representative of the i_{an} requirement featuring paints at their mid age between launch and drydocking. Keeping in mind that in laboratory tests $i_{an} = 40 \text{ mA cm}^{-2}$ onset “pH = 3/free-Cl 3–6 ppm” conditions near the anode (the harshest in the pH/free-Cl matrix) which determined the detachment phenomena, for the examined FR and SP paints, it can be argued that the probability of paint detachment occurring at the anode/paint interface is higher in the second half of the period between the launch and the drydocking. In

addition, whenever these i_{an} values are reached, the probability of paint detachment tends to be lowered in relation to the increase in sailing vs mooring stages; convection related to sailing stages modifies the acidity and chlorination concentration gradients near the anodes driving to milder pH/free-Cl conditions.

Finally, it can be summarized that

- in laboratory tests, the harshest “pH = 3/free-Cl 3–6 ppm” condition is found to be the only necessary requirement for the detachment to occur on both FR and SP paints,
- in real scenarios, the probability of appearance of these pH/free-Cl conditions increases when the protection current need overwhelms $i_{an} \approx 40 \text{ mA cm}^{-2}$, with mooring stages acting as an accelerating factor.

In addition, laboratory tests have showed that in mild pH/free-Cl conditions secondary effects, such as slight thinning and contact angle decrease, are likely to occur even in the absence of detaching phenomena. Looking at Fig. 1, these effects would be expected to extend over the anode/paint interface. For the sake of knowledge, it can be asked whether these effects are able to induce locally an attenuation of the foul control properties.

Conclusions

Concerning the behavior of new-generation biocide-free paints for ship hulls near ICCP anodes, where seawater turns acidic and chlorinated, a foul release and an amphiphilic self-polishing paint were exposed for three months in nine different pH/free-Cl conditions. The pH/free-Cl values were derived by a galvanostatic test run at an anodic current density representative of paints mid-aged between the launch and drydocking. Both paints detached only in harsh pH/free-Cl condition of the testing matrix; on the other hand, they showed thickness diminution and CA reduction in milder pH/free-Cl conditions, where no detachment was observed. These results enhance the knowledge about FR and SP paints in this stressing condition and help to figure out the behavior of the selected paints in real applications. Regarding the FR and SP paints here investigated, since (i) the paint detachment near ICCP anodes is a local issue and (ii) protecting currents are delivered at a growing intensity in relation to paint aging, the detachment of the coatings is supposed to occur at about 40% of the anode current supply threshold. This percentage features generally mid-aged paints. In addition, an important delaying factor of detachment is represented by larger $\frac{\text{mooring+sailing}}{\text{mooring}}$ ratios, reducing the concentration of anodic by-products and the probability of their permeation through the paints.

Acknowledgments This study was supported by operation cod. RLOF18ASSRIC/75/1 ‘Marine biocorrosion: study of interaction between new generation active and passive (biocide-free foul control coating) protection systems’ over the POR FSE Liguria 2014-2020—Axis 3 ‘Education and Training,’ Specific Objective 10.5—CUP G34I18000130009. Other partners of this project were ACG—Azienda Chimica Genovese s.r.l., (Genova, Italy) and Sinko Mec Kolor s.p.a., (Genova, Italy). The authors would also like to thank prof. Elisabetta Finocchio for her advice on FTIR spectra.

Funding Open access funding provided by Università degli Studi di Genova within the CRUI-CARE Agreement.

Open Access This article is licensed under a Creative Commons Attribution 4.0 International License, which permits use, sharing, adaptation, distribution and reproduction in any medium or format, as long as you give appropriate credit to the original author(s) and the source, provide a link to the Creative Commons licence, and indicate if changes were made. The images or other third party material in this article are included in the article’s Creative Commons licence, unless indicated otherwise in a credit line to the material. If material is not included in the article’s Creative Commons licence and your intended use is not permitted by statutory regulation or exceeds the permitted use, you will need to obtain permission directly from the copyright holder. To view a copy of this licence, visit <http://creativecommons.org/licenses/by/4.0/>.

References

1. Thiel, C, Broecheler, C, Ludwar, F, Rennings, A, Doose, J, Erni, D, “A Simple Superposition Formulation to Predict the Underwater Electric Potential Signature of Naval Vessels.” *J. Mar. Sci. Eng.*, **8** 105 (2020)
2. Flemming, HC, Murthy, PS, Venkatesan, R., Cooksey, K.E. (eds.) *Marine and Industrial Biofouling, Springer Series on Biofilms*. Springer, Berlin (2009)
3. Laidlaw, FB, “The History of the Prevention of Fouling.” *Proceedings of U.S. Naval Institute*, 78, 593 (1952)
4. Hakim, M, “Review of Correlation Between Marine Fouling and Fuel Consumption on a Ship” (2018).
5. Dafforn, KA, Lewis, JA, Johnston, EL, “Antifouling Strategies: History and Regulation, Ecological Impacts and Mitigation.” *Mar. Pollut. Bull.*, **62**, 453–465 (2011)
6. IMO, “Treaty Document 110-13—International Convention on Control of Harmful Anti-Fouling Systems on Ships, 2001”, Legislation, 2008, 01/22/2008 - 09/26/2008, <http://www.congress.gov/>.
7. Paz-Villarraga, CA, Braga, Castro I, Fillmann, G, “Biocides in Antifouling Paint Formulations Currently Registered for Use.” *Environ. Sci. Pollut. Res. Int.*, **29** 30090–30101 (2022)

8. Jin, H, Tian, L, Bing, W, Zhao, J, Ren, L, “Bioinspired Marine Antifouling Coatings: Status, Prospects, and Future.” *Prog. Mater. Sci.*, **124** 100889 (2022)
9. Qiu, H, Feng, F, Gapeeva, A, Meurisch, K, Kaps, S, Li, X, Yu, L, Mishra, YK, Adelung, R, Baum, M, “Functional Polymer Materials for Modern Marine Biofouling Control.” *Prog. Polymer Sci.*, **127** 101516 (2022)
10. Tian, L, Yin, Y, Bing, W, Jin, E, “Antifouling Technology Trends in Marine Environmental Protection.” *J. Bionic Eng.*, **18** 239–263 (2021)
11. Candries, M, Atlar, M, Anderson CD, “Foul Release Systems and Drag. Consolidation of Technical Advances in the Protective and Marine Coatings Industry;” *Proceedings of the PCE 2001 Conference*, pp. 273-286 (2001)
12. Lejars, M, Margaillan, A, Bressy, C, “Fouling Release Coatings: A Nontoxic Alternative to Biocidal Antifouling Coatings.” *Chem. Rev.*, **112** 4347–3490 (2012)
13. Han, X, Wu, J, Zhang, X, Shi, J, Wei, J, Yang, Y, Wu, B, Feng Y, “Special Issue on Advanced Corrosion-Resistance Materials and Emerging Applications. The Progress on Antifouling Organic Coating: From Biocide to Biomimetic Surface.” *J. Mater. Sci. Technol.* **61**, 46–62 (2021)
14. Benedetti, A, Castelli, F, Stifanese, R, Traverso, PL, Faimali, M, Bergo, A, Delucchi, M, “Cathodic Disbonding Tests Operating at Large Cathodic Potentials for Long Periods Need Current Monitoring, pH Control and Anode Isolation.” *Mater. Corros.*, **73** 1943–1953 (2022)
15. Bi, H, Sykes, J, “Cathodic Disbonding of an Unpigmented Epoxy Coating on Mild Steel Under Semi- and Full-Immersion Conditions.” *Corros. Sci.*, **53** 3416–3425 (2011)
16. Kuang, D, Cheng, YF, “Study of Cathodic Protection Shielding Under Coating Disbondment on Pipelines.” *Corros. Sci.*, **99** 249–257 (2015)
17. Shreepathi, S, “Physicochemical Parameters Influencing the Testing of Cathodic Delamination Resistance of High Build Pigmented Epoxy Coating.” *Prog. Org. Coat.*, **90** 438–447 (2016)
18. Tsehaye, MT, Velizarov, S, Van der Bruggen, B, “Stability of Polyethersulfone Membranes to Oxidative Agents: A Review.” *Polymer Degrad. Stab.*, **157** 15–33 (2018)
19. Davidson, RG, “Polymer Degradation Studies by FTIR.” *Prog. Pacific Polym. Sci.* **2**, 101–111 (1992)
20. Lindholdt, A, Dam-Johansen, K, Olsen, SM, Yebra, DM, Kiil, S, “Effects of Biofouling Development on Drag Forces of Hull Coatings for Ocean-Going Ships: A Review.” *J. Coat. Technol. Res.*, **12** 415–444 (2015)
21. Samarth, NB, Mahanwar, PA, “Degradation of Polymer & Elastomer Exposed to Chlorinated Water—A Review.” *Open J. Org. Polymer Mater.*, **11** 1–50 (2021)
22. Rahimi, A, Stafslie, SJ, Vanderwal, L, Finlay, JA, Clare, AS, Webster, DC, “Amphiphilic Zwitterionic-PDMS-Based Surface-Modifying Additives to Tune Fouling-Release of Siloxane-Polyurethane Marine Coatings.” *Prog. Org. Coat.*, **149** 105931 (2020)
23. Xu, L, Xin, Y, Ma, L, Zhang, H, Lin, Z, Li, X, “Challenges and Solutions of Cathodic Protection for Marine Ships.” *Corros. Commun.*, **2** 33–40 (2021)
24. Stalder, AF, Melchior, T, Müller, M, Sage, D, Blu, T, Unser, M, “Low-Bond Axisymmetric Drop Shape Analysis for Surface Tension and Contact Angle Measurements of Sessile Drops.” *Colloids Surfaces A Physicochem. Eng. Asp.*, **364** 72–81 (2010)
25. Eigeldinger, J, Vogt, H, “The Bubble Coverage of Gas-Evolving Electrodes in a Flowing Electrolyte.” *Electrochim. Acta*, **45** 4449–4456 (2000)

26. Gabrielli, C, Huet, F, Nogueira, RP, “Fluctuations of Concentration Overpotential Generated at Gas-Evolving Electrodes.” *Electrochim. Acta*, **50** 3726–3736 (2005)
27. Vogt, H, Balzer, RJ, “The Bubble Coverage of Gas-Evolving Electrodes in Stagnant Electrolytes.” *Electrochim. Acta*, **50** 2073–2079 (2005)
28. Tirumkudulu, MS, Punati, VS, “Solventborne Polymer Coatings: Drying, Film Formation, Stress Evolution and Failure.” *Langmuir*, **38** 2409–2414 (2022)
29. van der Kooij, HM, Sprakel, J, “Watching Paint Dry; More Exciting than it Seems.” *Soft. Matter*, **11** 6353–6359 (2015)
30. Tanaka, H, Komoda, Y, Horie, T, Ohmura, N, “Stress Development of Latex Coatings in a Convection Drying with the Accumulation and Deformation of Polymer Particles.” *Prog. Org. Coat.*, **170** 106941 (2022)
31. Kiil, S, Weinell, CE, Pedersen, MS, Dam-Johansen, K, “Analysis of Self-Polishing Antifouling Paints Using Rotary Experiments and Mathematical Modeling.” *Ind. Eng. Chem. Res.*, **40** 3906–3920 (2001)
32. Al-Borno, A, Brown, M, Rao, S, “The Effect of Anode Isolation Methods on Coating Cathodic Disbondment.” Paper n. 08007 by NACE International (2008)
33. Zhang, Y, Wang, J, Gao, F, Tao, H, Chen, Y, Zhang, H, “Impact of Sodium Hypochlorite (NaClO) on Polysulfone (PSF) Ultrafiltration Membranes: The Evolution of Membrane Performance and Fouling Behaviour.” *Sep. Purif. Technol.*, **175** 238–247 (2017)
34. Mikdam, A, Colin, X, Minard, G, Billon, N, Maurin, R, “A Kinetic Model for Predicting the Oxidative Degradation of Additive Free Polyethylene in Bleach Disinfected Water.” *Polym. Degrad. Stab.*, **14** 78–94 (2017)
35. Arkhangelsky, E, Kuzmenko, D, Gitis, V, “Impact of Chemical Cleaning on Properties and Functioning of Polyethersulfone Membranes.” *J. Membrane Sci.*, **305** 176–184 (2007)
36. Regula, C, Carretier, E, Wyart, Y, Ge san-Guiziu, G, Vincent, A, Boudot, D, Moulin, P, “Chemical Cleaning/Disinfection and Ageing of Organic UF Membranes: A Review.” *Water Res.*, **56** 325–365 (2014)
37. Tilahun Tsehay, M, Velizarov, S, Van der Bruggen, B, “Stability of Polyethersulfone Membranes to Oxidative Agents: A Review.” *Polym. Degrad. Stab.*, **157** 15–33 (2018)
38. Wang, J, Li, S, Guan, Y, Zhu, C, Gong, G, Hu, Y, “Novel RO Membranes Fabricated by Grafting Sulfonamide Group: Improving Water Permeability, Fouling Resistance and Chlorine Resistant Performance.” *J. Membrane Sci.*, **641** 119919 (2022)
39. Devilliers, C, Fayolle, B, Laiarinandrasana, L, Oberti, S, Gaudichet-Maurin, E, “Kinetics of Chlorine-Induced Polyethylene Degradation in Water Pipes.” *Polymer Degrad. Stab.*, **96** 1361–1368 (2011)
40. Awaja, F, Gilbert, M, Kelly, G, Fox, B, Pigram, PJ, “Adhesion of Polymers.” *Prog. Polymer Sci.*, **34** 948–968 (2009)
41. Mutsuda, M, Komada, H, “Direct Bonding Between Poly(oxy-2,6-dimethyl-1,4-phenylene) and Rubber with Radicals.” *J. Appl. Polym. Sci.*, **95** 53–59 (2005)
42. Callow, ME, Fletcher, RL, “The Influence of Low Surface Energy Materials on Bioadhesion a Review.” *Int. Biodeter. Biodegrad.*, **34** 333–348 (1994)
43. Rosenhahn, A, Schilp, S, Kreuzerc, HJ, Grunze, M, “The Role of “Inert” Surface Chemistry in Marine Biofouling Prevention.” *Phys. Chem. Chem. Phys.*, **17** 4275–4286 (2010)
44. Marmur, A, “Wetting on Hydrophobic Rough Surfaces: To Be Heterogeneous or Not To Be?” *Langmuir*, **19** 8343–8348 (2003)
45. Han, B, Liang, S, Wang, B, Zheng, J, Xied, X, Xiao, K, Wang, X, Huang, X, “Following Simultaneous Determination of Surface Energy and Roughness of Dense Membranes by a Modified Contact Angle Method.” *Colloids Surf. A*, **562** 370–376 (2019)
46. Gan, X, Lin, T, Jiang, F, Zhang, X, “Impacts on Characteristics and Effluent Safety of PVDF Ultrafiltration Membranes Aged by Different Chemical Cleaning Types.” *J. Membrane Sci.*, **640** 119770 (2021)
47. Susanto, H, Ulbricht, M, “Characteristics, Performance and Stability of Polyethersulfone Ultrafiltration Membranes Prepared by Phase Separation Method Using Different Macromolecular Additives.” *J. Membrane Sci.*, **327** 125–135 (2009)
48. Good, RJ, Van Oss, CJ, *Modern Approaches to Wettability*. In Schrader ME, Loeb GL (eds.) Plenum Press, New York (1992)
49. Yolsal, U, Horton, TAR, Wang, M, Shaver, MP, “Polymer-Supported Lewis Acids and Bases: Synthesis and Applications.” *Prog. Polymer Sci.*, **111** 101313 (2020)

Publisher’s Note Springer Nature remains neutral with regard to jurisdictional claims in published maps and institutional affiliations.